EUROPEAN ORGANIZATION FOR NUCLEAR RESEARCH

CERN–PPE/96-160
21 Oct. 1996

High-Precision Structural Studies of the Antiprotonic Helium Atom $\bar{p}^4He^+$ by Observing Laser Resonances with $\Delta v = \Delta(n - l - 1) = 2$

T. Yamazaki[1)], E. Widmann and J. Eades
CERN, CH-1211 Geneva 23, Switzerland

M. Kumakura and N. Morita
Institute for Molecular Science
Myodaiji, Okazaki 444, Japan

H.A. Torii, M. Hori, T. Ishikawa, F.E. Maas[2)], H. Tamura and R.S. Hayano
Department of Physics, University of Tokyo
7-3-1 Hongo, Bunkyo-ku, Tokyo 113, Japan

I. Sugai and Y. Fujita
Institute for Nuclear Study, University of Tokyo
3-2-1 Midori-cho, Tanashi, Tokyo 188, Japan

B. Ketzer, H. Daniel, F.J. Hartmann M. Hasinoff[3)], R. Pohl, R. Schmidt and T. von Egidy
Physik-Department, Technische Universität München
D-85747 Garching, Germany

D. Horváth
KFKI Research Institute for Particle and Nuclear Physics
H-1525 Budapest, Hungary

PS205 collaboration

Abstract

Very weak laser resonances of unfavoured transitions $(n, l) \to (n + 1, l - 1)$ have been observed in metastable $\bar{p}^4He^+$ atoms by using a pulsed antiproton beam. The observed wavelengths (713.578 ± 0.006 nm for $l = 34$ and 726.095 ± 0.004 nm for $l = 35$), as well as those of the known favoured transitions, are to a few ppm accounted for by a recent variational calculation of Korobov, which includes the relativistic correction.

submitted to Physical Review Letters

[1)] Permanent address: Institute for Nuclear Study, University of Tokyo, 3-2-1 Midori-cho, Tanashi, Tokyo 188, Japan

[2)] Present address, Institut für Kernphysik, Universität Mainz, D-55099 Mainz, Germany.

[3)] On leave of absence from Department of Physics, University of British Columbia, Vancouver, Canada

Since the discovery of the anomalous longevity of antiprotons against annihilation in liquid helium [1] comprehensive studies of this interesting phenomenon have been made at LEAR (Low Energy Antiproton Ring) of CERN [2, 3, 4, 5, 6]. With the advent of laser resonance spectroscopy of antiprotonic helium atoms $\bar{p}He^+$ [7, 8, 9, 10, 11] our microscopic understanding of this phenomenon in terms of individual states of large quantum numbers (n, l) has been definitely established to be in accordance with previous theoretical expectations [12, 13]. So far, we have detected the three resonances in ^{4}He and the two in ^{3}He, listed in Table 1. The method used [14] involved laser stimulation of the last radiative transition (metastable parent to a short-lived daughter) in a sequence or band of transitions with constant "vibrational" quantum number (or equivalently, radial node number) $v = n - l - 1$. In this way we have established the individual level lifetimes and initial populations of the bands with v=3 and v=2. However the technique is not restricted to $\Delta v = 0$ transitions, and the present paper reports our first successes in stimulating very weak transitions of the "interband " type in which $(n, l) \to (n + 1, l - 1)$, so that $\Delta v = 2$. As $\Delta v = 0$ transitions alone do not determine energy differences between bands of differing v, these experiments mark a new departure in the elucidation of the structure of the metastable $\bar{p}He^+$ atom. What is perhaps more important is that in conjunction with recent theoretical developments, they bring it into an arena where it plays the role of a laboratory for the study of the quantum electrodynamics of the antiproton.

Recently, the wavelengths of all measured $\Delta v = 0$ transitions have been accounted for at the 50 ppm level by a large-configuration molecular-expansion variational calculation of the $\bar{p}He^+$ energy levels made by Korobov [15]. More recently, Korobov has calculated the shifts produced in the levels when relativistic corrections are included in the motion of the bound electron [16], with the results that the experimental transition wavelengths are now in agreement with his calculated values to a few ppm. The $\Delta v = 2$ transitions reported below bring further confirmation of the accuracy of this theoretical approach. As a selection rule favours transitions with the largest overlap of radial wavefunctions with the same node [12, 13], the strength of the $\Delta v = 2$ transitions was expected to be smaller by two orders of magnitude than that of the $\Delta v = 0$ transitions [14]. We shall sometimes therefore refer to them as "unfavoured" transitions, and to the $\Delta v = 0$ ones as "favoured" ones.

For the experiments on these transitions we developed a novel experimental technique in which pulsed antiprotons created a large number of metastable $\bar{p}He^+$ atoms almost instantaneously. These were then collectively illuminated with a single laser pulse. This differs from our previous experiments in which a continuous $\bar{p}$ beam was used and the laser pulse was applied every time a metastable $\bar{p}He^+$ atom was known to have been formed in a helium target. In the present case, antiprotons of 200 MeV/c momentum were extracted from the LEAR storage ring in the form of a train of 200ns-wide pulses. The initial pulse of each train contained some $10^7 - 10^8$ particles, while subsequent ones decreased exponentially in intensity as the ring was emptied. Each pulse was ejected from the ring on receipt of a master command generated from the experiment, and was brought to rest in the helium gas target. The intensity and position of the $\bar{p}$ beam were monitored with a parallel-plate ionization chamber with x and y readouts of 1.5 mm resolution, which indicated a beam spot size of 4 mm x 4 mm. The target was refrigerated to about 6 K and maintained at pressures near 500 mbar. Under these conditions, the antiprotons stopped in a region with cross section of 1 cm^2 and a length of some 5 cm, and produced between 3×10^5 and 3×10^6 metastable $\bar{p}He^+$ atoms.

These annihilated over a period of several microseconds, producing via their annihilation pions a light pulse of similar duration in a nearby Lucite Cerenkov radiator. This was preceded by a sharp initial flash of light from the 97 % fraction of the antiproton pulse that annihilated instantaneously. Superimposed on this time spectrum was the background light from $\pi^+ - \mu^+ - e^+$ decays produced by those annihilation pions that stopped in the cryostat wall and other material surrounding the helium target. The composite light pulse was viewed by a photomultiplier tube the second and fourth dynodes of which were gated to suppress the initial prompt annihilation [17]. The shape of the resulting current pulse was thus an analogue of the delayed annihilation time spectrum but included the $\pi^+ - \mu^+ - e^+$ decay background mentioned above. This pulse is referred to in what follows as the Analogue Delayed Annihilation Time Spectrum (ADATS).

The $\bar{p}$ stopping region was illuminated by the laser pulse at a suitable time (0.5 μs or more) after the $\bar{p}$ beam pulse arrived. When the laser was on a given resonance, most of the metastable atoms in the corresponding parent state could be forced to annihilate, as described in [14] for the continuous $\bar{p}$ case. This collective annihilation produced an easily detectable flash of Cerenkov light superimposed on the continuous ADATS. For the same number of resonance events in the continuous $\bar{p}$ beam mode we would, of course, have had to apply some 10^6 laser pulses, one for each delayed event.

The laser system used was essentially the same (except for the trigger mode) as in our previous experiments [7, 8, 9]. A combination of excimer and dye lasers produced light pulses of some 30 ns length. The excimer laser and the kicker magnet that ejected the $\bar{p}$ pulse from LEAR were fired with a suitable relative time delay by the common master command pulse. In practice a series of excimer trigger pulses was sent for 3 seconds before each master command to warm up the lasers and assure constant laser power and timing stability. The laser power used was about 3 mJ per pulse.

We tuned the laser light to the ''red" region to search for the two candidates from the $n = 37$ states near values 713.54 nm (for $(37, 34) \rightarrow (38, 33)$) and 726.02 nm (for $(37, 35) \rightarrow (38, 34)$). These were the values predicted from the calculation of Korobov mentioned above [15]. In fact, we found the 726 nm resonance almost immediately. Fig.1a shows a single pulse ADATS when the laser was tuned to 726.096 nm. The resonance spike is very clear with an overwhelming statistical significance, though the peak to background ratio was not large. The measured resonance profile is shown in Fig.1b and has a central vacuum wavelength of 726.095 ± 0.004 nm. The error includes the wavelength calibration error of $\pm$ 0.003 nm.

We then searched for the $(37, 34) \rightarrow (38, 33)$ resonance, which turned out to be more difficult. Fig.1c shows an ADATS when the laser was tuned to 713.588 nm, at which a small but significant spike appeared at 0.96 μs. The resonance profile measured (Fig.1d) shows a very broad peak. Its FWHM width (fitted by a Lorentzian) is 0.067 ± 0.006 nm (94 ppm), which is much larger than the laser bandwidth of 0.007 nm. The central wavelength was determined to be 713.578 ± 0.006 nm.

Its broadness may be explained in terms of a large natural width of the v=4 (38,33) daughter state. This has the unusual feature that it undergoes an L (multipolarity) = $\Delta l = 2$ Auger transition and can therefore be expected to have a lifetime in the 10 ps range, while all the other daughter states so far observed are located at the metastability boundary, and should have the 10 ns lifetimes characteristic of $L = 3$ Auger transitions. We deduce the lifetime of the (38,33) state to be 4.1 ± 0.2 ps, which is consistent with the above expectation. Very recent calculations of the Auger transition rates by Korobov [18] and by Kartavtsev [19] give a decay lifetime of 3.2 ps and 5 ps, respectively, which agree excellently with the present observation.

The established level sequence is presented in Fig.2 (upper), and all the resonance transitions so far observed are summarized in Table 1, where the theoretical values of Korobov (both non-relativistic [15] and relativistic [16]) are also listed for comparison. The deviations of the theoretical wavelengths (λ_{theor}) from the experimental ones (λ_{exp}), are shown in Fig.2 (lower). From the comparison we observe the following characteristics.

i) While the earlier theoretical values [12, 13, 20, 21] scatter and deviate by the order of 1000 ppm from the experimental values, Korobov's non-relativistic values [15] are generally in excellent agreement with the experimental ones, although they are systematically shifted toward shorter wavelengths as much as 50-100 ppm. While the deviations for "intraband" ($\Delta v = 0$) transitions are about 50 ppm, those for the "interband" ($\Delta v = 2$) transitions are about 100 ppm.

ii) The relativistic corrections for the bound electron by Korobov [16] are all toward the longer wavelength direction and are state dependent. This is because the effective nuclear charge felt by the bound electron (and thus its velocity) depends on the spatial distribution of the $\bar{\mathrm{p}}$. The relativistic corrections are typically 50 ppm and 100 ppm for $\Delta v = 0$ and $\Delta v = 2$ transition, respectively. The final theoretical values both for the $\Delta v = 0$ and $\Delta v = 2$ transitions are surprisingly close to the experimental values (*i.e.*, within several ppm) and are all in the same direction, suggesting that calculations of higher order terms will bring still better agreement.

iii) Since the daughter state (38,33) of the 714 nm broad resonance is very short lived and is located far outside the metastable zone, it should provide the most stringent test of the applicability of the theoretical treatment on such unstable states. The difference between the Korobov value with the relativistic correction and the experimental one in the broad resonance transition is somewhat larger than in the other $\Delta v = 2$ transition (726 nm). The deviation of 21 ppm, however, appears remarkably small in consideration of the broadness (94 ppm FWHM width) of the daughter state.

Thus we have developed a new method to study extremely weak $\Delta v = 2$ transitions using a pulsed antiproton beam and observed two such resonances. The results have revealed the importance of the state-dependent relativistic corrections included by Korobov in his variational calculation of metastable $\bar{\mathrm{p}}\mathrm{He}^+$ levels [15, 16]. The difference between theory and experiment for all the wavelengths so far observed is only several ppm (except for the broad resonance case) when the relativistic corrections to the electron motion are taken into account. The constant sign of these discrepancies implies that closer and closer constraints are being placed on the principal scaling factor for all transitions (the antiproton equivalent of the Rydberg constant), while their small magnitude indicates that our measurements are now testing the fundamental properties of the antiproton as well as few-body theories. In view of further theoretical developments to be expected in the near future it is very important to achieve higher and higher experimental precisions. Even small pressure shifts of the resonance wavelengths must be studied and corrected for.

We are indebted to the LEAR and PS staff at CERN (in particular to Michel Chanel) for their tireless dedication in providing us with the fast extracted antiproton beam. We also thank V.I. Korobov for making his theoretical results available to us prior to publication. The present work is supported by the Grants-in-Aid for Specially Promoted

Research and for International Scientific Research of the Japanese Ministry of Education, Science and Culture, the Bundesministerium für Bildung, Wissenschaft, Forschung und Technologie and the Hungarian National Science Foundation. H.A.T acknowledges the support of Japan Society for the Promotion of Science.

References

[1] M. Iwasaki *et al.*, Phys. Rev. Lett. 67, 1246 (1991).
[2] T. Yamazaki et al., Nature 361, 238 (1993).
[3] S.N. Nakamura *et al.*, Phys. Rev. A49, 4457 (1994).
[4] E. Widmann *et al.*, Phys. Rev. A51, 2870 (1995).
[5] E. Widmann *et al.*, Phys. Rev. A53, 3129 (1996).
[6] B. Ketzer *et al.*, Phys. Rev. A53, 2108 (1996).
[7] N. Morita *et al.*, Phys. Rev. Lett. 72, 1180 (1994).
[8] R.S. Hayano *et al.*, Phys. Rev. Lett.73, 1485 (1994); 73, 3181(E) (1994).
[9] F.E. Maas *et al.*, Phys. Rev. A52, 4266 (1995).
[10] H.A. Torii *et al.*, Phys. Rev. A53, R1931 (1996).
[11] R.S. Hayano *et al.*, *to be submitted*
[12] T. Yamazaki and K. Ohtsuki, Phys. Rev. A45, 7782 (1992).
[13] I. Shimamura, Phys. Rev. A46, 3776 (1992).
[14] N. Morita, K. Ohtsuki and T. Yamazaki, Nucl. Instr. Meth. A330, 439 (1993).
[15] V.I. Korobov, Phys. Rev. A, *in press.*
[16] V.I. Korobov, *prepared for publication (January 1996).*
[17] A. Niestroj *et al.*, Nucl. Instr. Methds A373, 411 (1996).
[18] V.I. Korobov, *private communication (March, 1996)*
[19] O. Kartavtsev, *private communication (March, 1996)*
[20] O. Kartavtsev, *private communication (1994).*
[21] Y. Kino, *private communication (1993).*

Table 1. Comparison of the observed transition wavelengths λ_{exp} with the theoretical prediction of Korobov λ_{theor} (A: without relativistic corrections [15]; B: with relativistic corrections. [16]) The errors reflect the experimental uncertainties only.

Isotope	Δv	$(n_i, l_i) \to (n_f, l_f)$	λ_{exp}	λ_{theor}		$(\lambda_{theor} - \lambda_{exp})/\lambda_{exp}$		Ref
			(nm)	A (nm)	B (nm)	A (ppm)	B (ppm)	
^{4}He	0	$(39, 35) \to (38, 34)$	597.259(2)	597.229	597.262	-50 ± 3	+5.0 ± 3	[7]
^{4}He	0	$(38, 35) \to (37, 34)$	529.621(3)	529.596	529.623	-47 ± 6	+3.0 ± 6	[11]
^{4}He	0	$(37, 34) \to (36, 33)$	470.724(2)	470.705	470.725	-41 ± 4	+2.1 ± 4	[9]
^{3}He	0	$(38, 34) \to (37, 33)$	593.388(1)	593.360	593.394	-48 ± 2	+8.6 ± 2	[10]
^{3}He	0	$(36, 33) \to (35, 32)$	463.946(2)	463.928	463.949	-38 ± 4	+5.4 ± 4	[10]
^{4}He	2	$(37, 34) \to (38, 33)$	713.578(6)	713.515	713.594	-81 ± 9	+21.3 ± 9	Herein
^{4}He	2	$(37, 35) \to (38, 34)$	726.095(4)	726.021	726.102	-102 ± 6	+10.0 ± 6	Herein

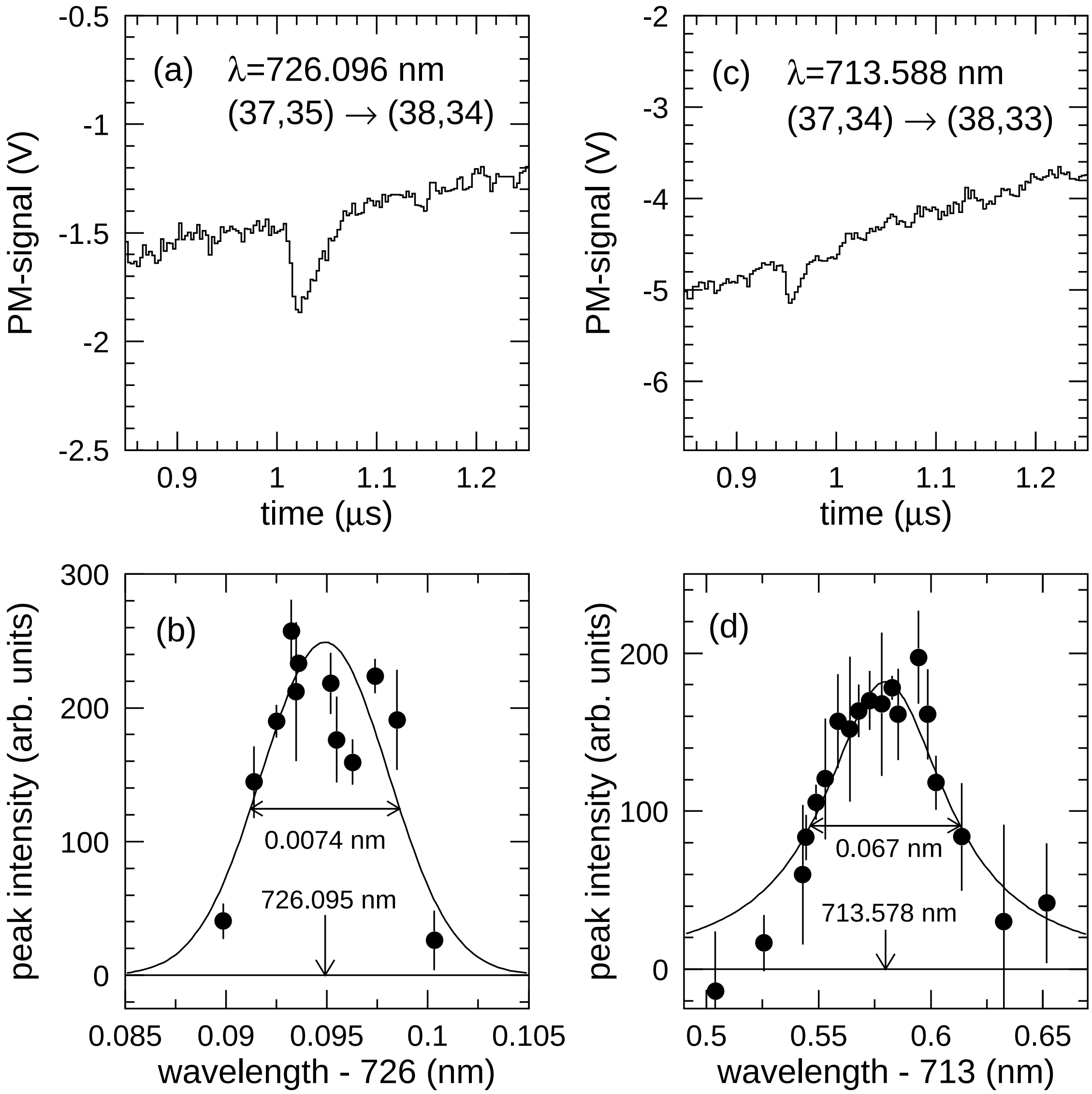

Figure 1: The 726 nm and 714 nm "unfavoured" resonance spikes in analog-DATS and their resonance profiles. a) Analog DATS showing a resonance spike at 726.096 nm. b) Resonance profile of the 726 nm transition. The vertical bars indicate variances of ADATS peak intensities after repeated measurements and a single Gausssian function is used to determine the central wavelength. c) Analog DATS showing a resonance spike at 713.588 nm. d) Resonance profile of the 714 nm transition.

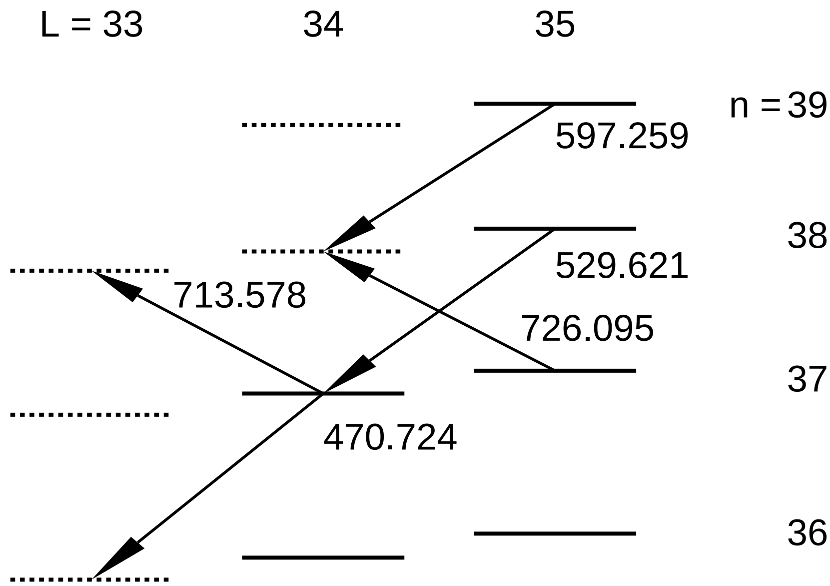

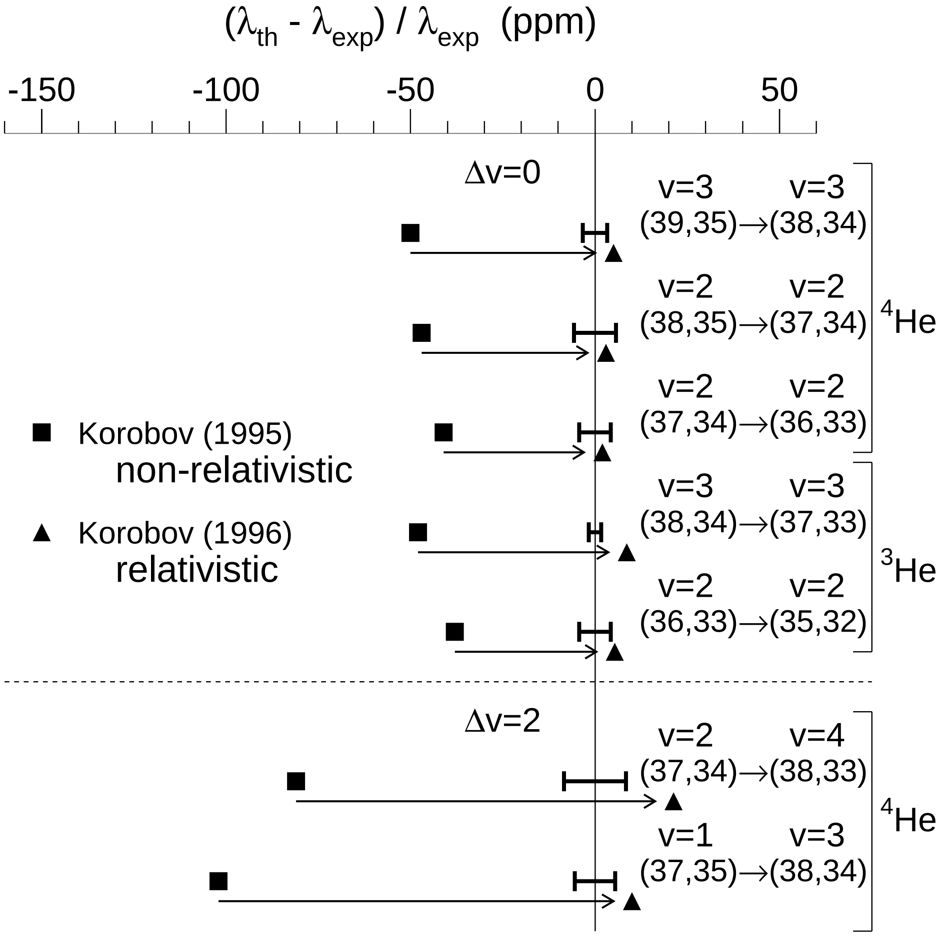

Figure 2: (Upper) Partial level scheme established by the present laser resonance spectroscopy. The observed resonance wavelenghts are shown. (Lower) Comparison of the experimental wavelengths of various transitions with Korobov predictions (closed squares without [15] and closed triangles with [16] relativistic corrections). The upper part is for $\Delta v = \Delta(n - l - 1) = 0$ intraband transitions and the lower part is for $\Delta v = 2$ interband transitions. The error bars are the experimental ones.